Title

Low- and high-grade glioma-associated vascular cells differentially regulate tumor growth

Journal

Molecular Cancer Research, 22(7)

ISSN

1541-7786

Authors

Muthukrishnan, Sree Deepthi
Qi, Haocheng
Wang, David
et al.

Publication Date

2024-07-02

DOI

10.1158/1541-7786.mcr-23-1069

Peer reviewed

Low- and High-Grade Glioma-Associated Vascular Cells Differentially Regulate Tumor Growth

Sree Deepthi Muthukrishnan[1,2], Haocheng Qi[1], David Wang[1], Lubayna Elahi[1], Amy Pham[1], Alvaro G. Alvarado[1], Tie Li[3], Fuying Gao[1], Riki Kawaguchi[1], Albert Lai[3], and Harley I. Kornblum[1,4]

ABSTRACT

A key feature distinguishing high-grade glioma (HG) from low-grade glioma (LG) is the extensive neovascularization and endothelial hyperproliferation. Prior work has shown that tumor-associated vasculature from HG is molecularly and functionally distinct from normal brain vasculature and expresses higher levels of protumorigenic factors that promote glioma growth and progression. However, it remains unclear whether vessels from LG also express protumorigenic factors, and to what extent they functionally contribute to glioma growth. Here, we profile the transcriptomes of glioma-associated vascular cells (GVC) from IDH-mutant (mIDH) LG and IDH-wild-type (wIDH) HG and show that they exhibit significant molecular and functional differences. LG-GVC show enrichment of extracellular matrix–related gene sets and sensitivity to antiangiogenic drugs, whereas HG-GVC display an increase in immune response–related gene sets and antiangiogenic resistance. Strikingly, conditioned media from LG-GVC inhibits the growth of wIDH glioblastoma cells, whereas HG-GVC promotes growth. *In vivo* cotransplantation of LG-GVC with tumor cells reduces growth, whereas HG-GVC enhances tumor growth in orthotopic xenografts. We identify ASPORIN (ASPN), a small leucine-rich repeat proteoglycan, highly enriched in LG-GVC as a growth suppressor of wIDH glioblastoma cells *in vitro* and *in vivo*. Together, these findings indicate that GVC from LG and HG are molecularly and functionally distinct and differentially regulate tumor growth.

Implications: This study demonstrated that vascular cells from IDH-mutant LG and IDH-wild-type HG exhibit distinct molecular signatures and have differential effects on tumor growth via regulation of ASPN-TGFβ1-GPM6A signaling.

Introduction

High-grade gliomas (HG, grade 4) are more extensively vascularized than low-grade gliomas (LG, grade 2/3), with endothelial hyperproliferation serving as a key histopathologic hallmark differentiating these tumors (1). Despite being highly angiogenic tumors, antiangiogenic therapies have largely been unsuccessful in impeding tumor growth or improving patient survival outcomes in HG. This resistance is mainly due to activation of alternative neovascularization mechanisms such as vessel co-option, vascular mimicry, vasculogenesis and endothelial transdifferentiation, and activation of other proangiogenic pathways (2, 3). Nevertheless, the neoplastic vessels generated by these mechanisms are highly dysfunctional, leaky, and disorganized. Prior studies including our work have demonstrated that glioma-associated vascular cells (GVC) from HG are molecularly heterogeneous compared with normal brain vascular cells (4–9).

The vasculature of LG is not well studied compared with HG. Importantly, the majority of adult LG have mutations in the enzyme Isocitrate dehydrogenase (IDH)1 or IDH2 with 50% to 80% reported in grade 2 and 54% in grade 3 gliomas (10). On the contrary, only 15% to 20% of grade 4 gliomas harbor mutations in IDH1 or IDH2, indicating that IDH mutation status may govern the vascular phenotype, and this could in turn influence their sensitivity to antiangiogenic therapies. A recent study reported key differences in angiogenic gene expression related to hypoxia and TGFβ signaling between LG (grade 2) IDH-wild-type and mutant tumor vessels (11). It remains undetermined to what extent the molecular landscape of vascular cells from LG differs from HG, and how it influences their response to antiangiogenic treatments, and whether the angiocrines expressed in LG-GVC exhibit protumorigenic functions.

In this study, we conducted transcriptomic profiling of GVC isolated and cultured from IDH-mutant (mIDH) grade 2/3 LG and IDH-wild-type (wIDH) grade 4 HG that included primary and recurrent tumors. We show LG- and HG-GVC exhibit significant molecular and functional heterogeneity and differential sensitivity to antiangiogenic therapy. LG and HG-GVC differentially regulate the growth of wIDH GBM *in vitro* and in orthotopic xenograft models. Differential gene-expression analysis revealed that several extracellular matrix proteins are enriched in LG-GVC and inflammatory cytokines and chemokines in HG-GVC. Specifically, we identified Asporin (ASPN), a member of the small leucine-rich proteoglycan family, highly enriched in LG-GVC as a potential tumor suppressor that differentially regulates the growth of wIDH and mIDH tumors via modulation of TGFβ1 signaling.

Materials and Methods

Patient-derived gliomasphere lines

All patient-derived gliomasphere lines used in this study were previously established in our laboratory. Gliomaspheres were

[1]Department of Psychiatry and Behavioral Sciences and the UCLA Intellectual and Developmental Disabilities Research Center, David Geffen School of Medicine, UCLA, Los Angeles, California. [2]Department of Oncology Science, College of Medicine, University of Oklahoma, Oklahoma City, Oklahoma. [3]Department of Neurology, David Geffen School of Medicine, UCLA, Los Angeles, California. [4]Department of Molecular and Medical Pharmacology, David Geffen School of Medicine, UCLA, Los Angeles, California.

Corresponding Authors: Harley I. Kornblum, Semel Institute of Neuroscience, University of California, Los Angeles, Room 375D NRB, Los Angeles, CA 90095. E-mail: hkornblum@mednet.ucla.edu; and Sree Deepthi Muthukrishnan, BSMB 937, 940 Stanton L Young Blvd, Oklahoma City, OK 73104. E-mail: sreedeepthi-muthukrishnan@ouhsc.edu

Mol Cancer Res 2024;22:656–67

doi: 10.1158/1541-7786.MCR-23-1069

cultured in DMEM/F12 medium supplemented with B27, 20 ng/mL bFGF, 50 ng/mL EGF, 5 μg/mL heparin, and antibiotics penicillin/streptomycin. Gliomaspheres were dissociated into single cells every 7 to 14 days depending on growth rate, and experiments were performed with cell lines that were cultured for <20 passages since their initial establishment and tested negative for mycoplasma contamination. Cell lines were authenticated by short tandem repeat analysis.

Culture of GVC and human brain microvascular endothelial cells

GVC (P1 to P9) and human brain microvascular endothelial cells (HBEC; Sciencell, 1000) were cultured in endothelial cell growth media (R&D Systems, CCM027) in tissue culture flasks. Validation of vascular identity was done using CD31 immunostaining at P2 and P7 after expansion. Detailed protocol for isolation of GVC from patient tissue is provided in Supplementary Methods.

RNA sequencing and analysis

Bulk RNA sequencing (RNA-seq) and single-cell RNA-seq (scRNA-seq) data set analysis was carried out as described previously and detailed in Supplementary Methods (8, 12). Information on patient samples used for sequencing is listed in Supplementary Table S5.

Animal strains, intracranial transplantation, and imaging

All animal studies were performed according to approved protocols by the Institutional Animal Care and Use Committee (IACUC) at UCLA. Studies did not discriminate sex, and both males and females were used. Strains: 10- to 12-week-old NOD-SCID gamma null mice were used to generate orthotopic xenografts. A total of 5×10^4 cells from a patient-derived GBM line (HK408) containing a firefly-luciferase-GFP lentiviral construct were injected intracranially into the neostriatum in mice. Cotransplantation with GVC-expressing mCherry was performed at a ratio of 1:1 (GBM: GVC), with 5×10^4 cells per condition. Imaging: Tumor growth was monitored 2 and 4 weeks after transplantation by measuring luciferase activity using IVIS Lumina II bioluminescence imaging. ROIs were selected to encompass the tumor area, and radiance was used as a measure of tumor burden.

Lentiviral constructs and gene knockdown

PLV-mCherry (Vector builder), shRNA-scrambled, shRNA-ASPN-GFP, and shRNA-GPM6A-GFP (abmgood) were purchased from manufacturers as indicated. Briefly, cells were transduced with the lentivirus, and reporter expression was analyzed at 48 hours. Following reporter activity, cells were selected with puromycin (Sigma-Aldrich, P8833) for 72 hours and knockdown of respective genes was confirmed by quantitative RT-PCR and Western blotting.

Statistical analysis

All data are expressed as the mean ± SD. *P* values were calculated in GraphPad Prism 8.0 using unpaired two-tailed Student *t* test and ANOVA for multiple comparisons followed by Bonferroni correction and *post hoc t* test. *P* values of less than 0.05 were considered significant. Log-rank analysis was used to determine the significance of Kaplan–Meier survival curves.

All other materials and methods are described in the Supplementary Methods. Graphical illustrations were generated using BioRender (http://biorender.com,RRID:SCR_018361).

Data availability

All sequencing data have been submitted to Gene-Expression Omnibus and are available with the accession number GSE236571.

Results

GVCs are molecularly distinct from normal brain endothelial cells

To determine whether GVCs exhibit molecular heterogeneity, we first isolated $CD31^+$ vascular and $CD31^-$ tumor cells from glioblastoma (GBM, grade 4) patients. Immunostaining and quantitative RT-PCR analysis of the two fractions showed enrichment of endothelial as well as some pericyte markers in the $CD31^+$ fraction indicating that they are a mixture of both the vascular cell types, hence being referred to as GVCs (**Fig. 1A** and **B**). RNA-seq and differential gene-expression analysis (DEA) of $CD31^-$ tumor and $CD31^+$ vascular fractions also showed significant enrichment of both endothelial and pericyte genes but not glioma stem cell (GSC) markers (**Fig. 1C**).

Next, to ensure that GVC maintained their vascular identity in long-term culture, we performed immunostaining for CD31 at early (P1–P2) and late (P5–P7) passages and found that the expression was maintained over several passages (Supplementary Fig. S1A). Further, we performed RNA-seq on early (P1–P2) and late (P4–P7) passage GVC isolated from two GBM patients and compared with cultured HBEC. Principal component analysis showed that GVC and HBEC clustered separately indicating that they are molecularly distinct (**Fig. 1D**). DEA also showed that cultured GVC are significantly distinct from HBEC, but there is minimal difference between early and late passage GVC cultures (Supplementary Fig. S1B). Gene set enrichment analysis (GSEA) revealed enrichment of cell-cycle and DNA-repair–related processes in GVC compared with HBEC (**Fig. 1E**). We also compared the gene-expression profiles of cultured and freshly isolated GVC and found that they closely clustered together (Supplementary Fig. S1C and S1D). Together, these data strongly indicate that GVC are molecularly distinct from HBEC.

LG- and HG-GVC display molecular and functional heterogeneity

Given that microvascular hyperproliferation is a distinguishing feature of grade 4 GBM, we wondered if GVC from LG and HG exhibited molecular and functional heterogeneity (2). To test this, we performed whole transcriptomic sequencing of GVC cultures derived from grade 2/3, mIDH LG ($N = 5$) and grade 4, wIDH primary ($N = 4$), and recurrent GBM ($N = 5$) patient samples. DEA revealed significantly higher transcriptomic differences between HG- and LG-GVC, but minimal differences between primary (PRI) and recurrent (REC)-GVC (**Fig. 2A** and **B**; Supplementary Table S1). GSEA showed that HG-GVC are significantly enriched for inflammatory cytokine-related gene sets, whereas LG-GVC are enriched for extracellular matrix-related gene sets (**Fig. 2C**; Supplementary Fig. S2A, Supplementary Tables S2 and S3). Consistent with prior findings, we found that both LG-GVC and HG-GVC are morphologically distinct from HBEC and displayed different rates of proliferation as assessed by EdU incorporation in culture (Supplementary Fig. S2B and S2C; refs. 4, 5, 11)). Both LG- and HG-GVC also showed greater migration capacity than HBEC (Supplementary Fig. S2D). HBEC and LG-GVC displayed higher sensitivity to antiangiogenic treatments including bevacizumab and sunitinib, whereas HG-GVC were resistant even at higher doses (**Fig. 2D** and **E**). Furthermore, GVC were highly resistant to high doses of radiation (8–10 Gy) compared with HBEC (Supplementary

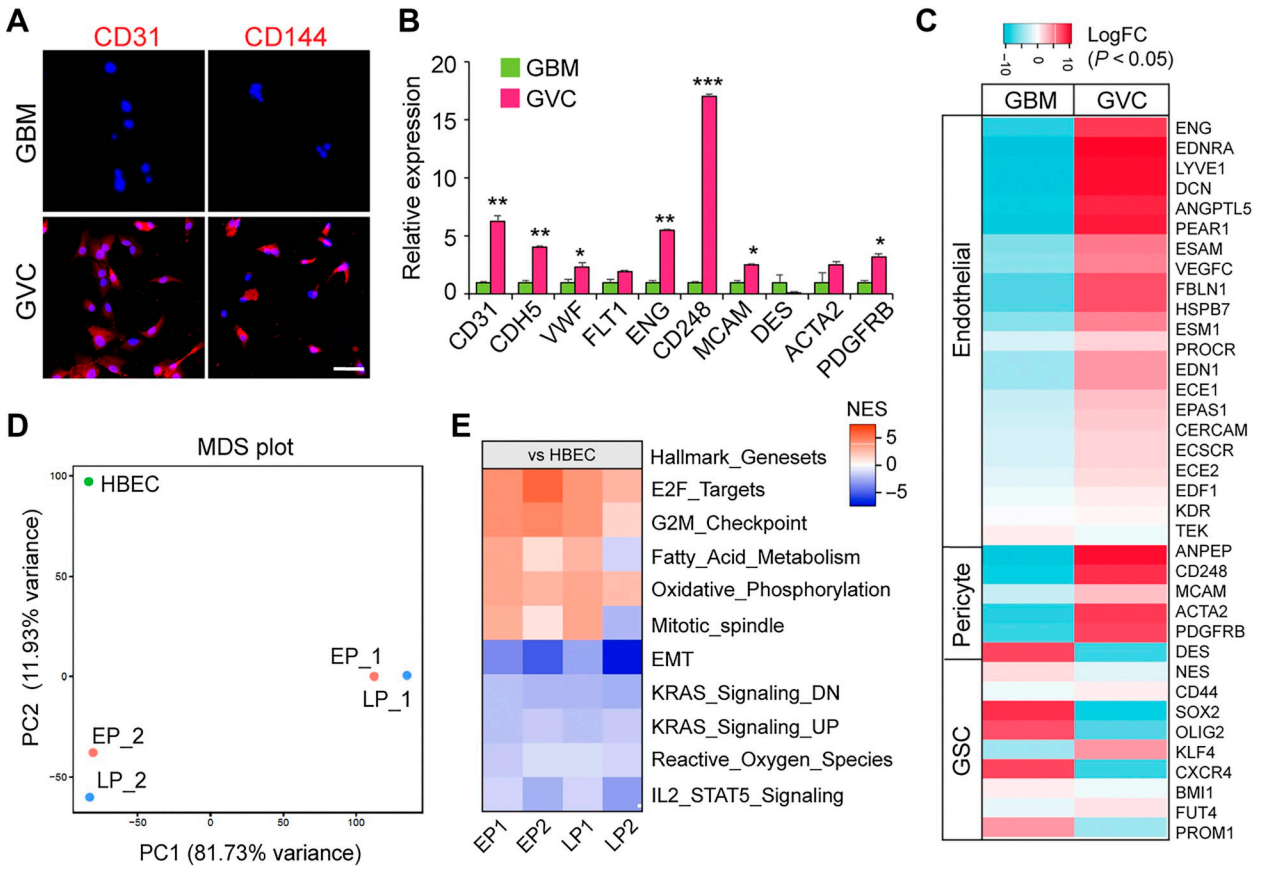

Figure 1.

Molecular differences between glioma-associated vascular cells and normal brain endothelial cells. **A,** Immunostaining of CD31 (red) and CD144 (VE-CADHERIN, red) and DAPI (nuclei, blue) in patient-derived GBM and GVC fractions. Scale bars, 100 μm. **B,** Relative expression of endothelial and pericyte markers in GBM and GVC fractions. $N = 3$, *, $P < 0.05$; **, $P < 0.005$; and ***, $P < 0.0005$, unpaired t test. **C,** Heat map of LogFc expression of endothelial, pericyte, and glioma stem cell (GSC) markers in GBM and GVC fractions. **D,** MDS plot of GVC cultured from early (EP) and late (LP) passages and HBEC (normal human brain microvascular endothelial cells). **E,** Heat map of gene sets enriched in early and late passage GVC compared with HBEC

Fig. S2E). These findings indicate that GVC from HG gliomas exhibit a greater capacity for treatment resistance than LG-GVC, and they are molecularly and functionally distinct from normal HBEC.

LG-GVC and HG-GVC differentially regulate the growth of wIDH GBM and mIDH astrocytoma

Based on the molecular and functional differences between LG- and HG-GVC, we postulated that they may differentially influence the growth of tumor cells. We therefore collected conditioned media (CM) from LG-, PRI-, and REC-GVC cultures to determine if they differentially regulate the growth of GBM cells. First, we tested the effects of GVC-CM on wIDH GBM lines (HK408, HK301, and HK336) and found that HG-GVC promoted whereas LG-GVC significantly inhibited the growth and viability of these tumor lines (**Fig. 3A** and **B**; Supplementary Fig. S3A). On the contrary, HG-GVC did not alter the growth of the mIDH astrocytoma line, whereas LG-GVC slightly promoted their growth, indicating that they differentially affect the growth and viability of wIDH GBM and mIDH astrocytoma tumor cells (**Fig. 3C**; Supplementary Fig. S3B).

To validate the *in vitro* findings, we performed cotransplantation of either LG- or HG-GVC along with wIDH GBM cells expressing firefly-luciferase-GFP into immunocompromised mice to generate orthotopic xenografts. Examination of tumors 4 weeks posttransplantation showed that LG-GVC significantly inhibited the growth of the tumor cells, whereas both PRI- and REC-GVC enhanced the growth of the tumors (**Fig. 3D** and **E**). This was also reflected in animal survival, as tumors cotransplanted with LG-GVC significantly survived longer, and mice bearing tumors with HG-GVC showed significantly reduced survival (**Fig. 3F**). These findings strongly suggest that LG- and HG-GVC differentially regulate wIDH GBM growth.

LG-GVC and HG-GVC show differential expression of extracellular matrix proteins, growth factors, and cytokines

To elucidate the mechanism underlying the differential effects of GVC on tumor growth, we examined the transcriptomic data for secreted factors differentially expressed between LG- and HG-GVC. Interestingly, we found several extracellular matrix proteins enriched in LG-GVC that were either not expressed or showed minimal expression in HG-GVC. Similarly, we found increased expression of chemokines and cytokines in HG-GVC that showed virtually little to no expression in LG-GVC. We also verified that these transcripts were enriched in GVC relative to HBEC (**Fig. 4A**; Supplementary Table S4).

Furthermore, we examined previously published bulk RNA-seq data of freshly isolated $CD31^+$ GVC from primary GBM tumors and

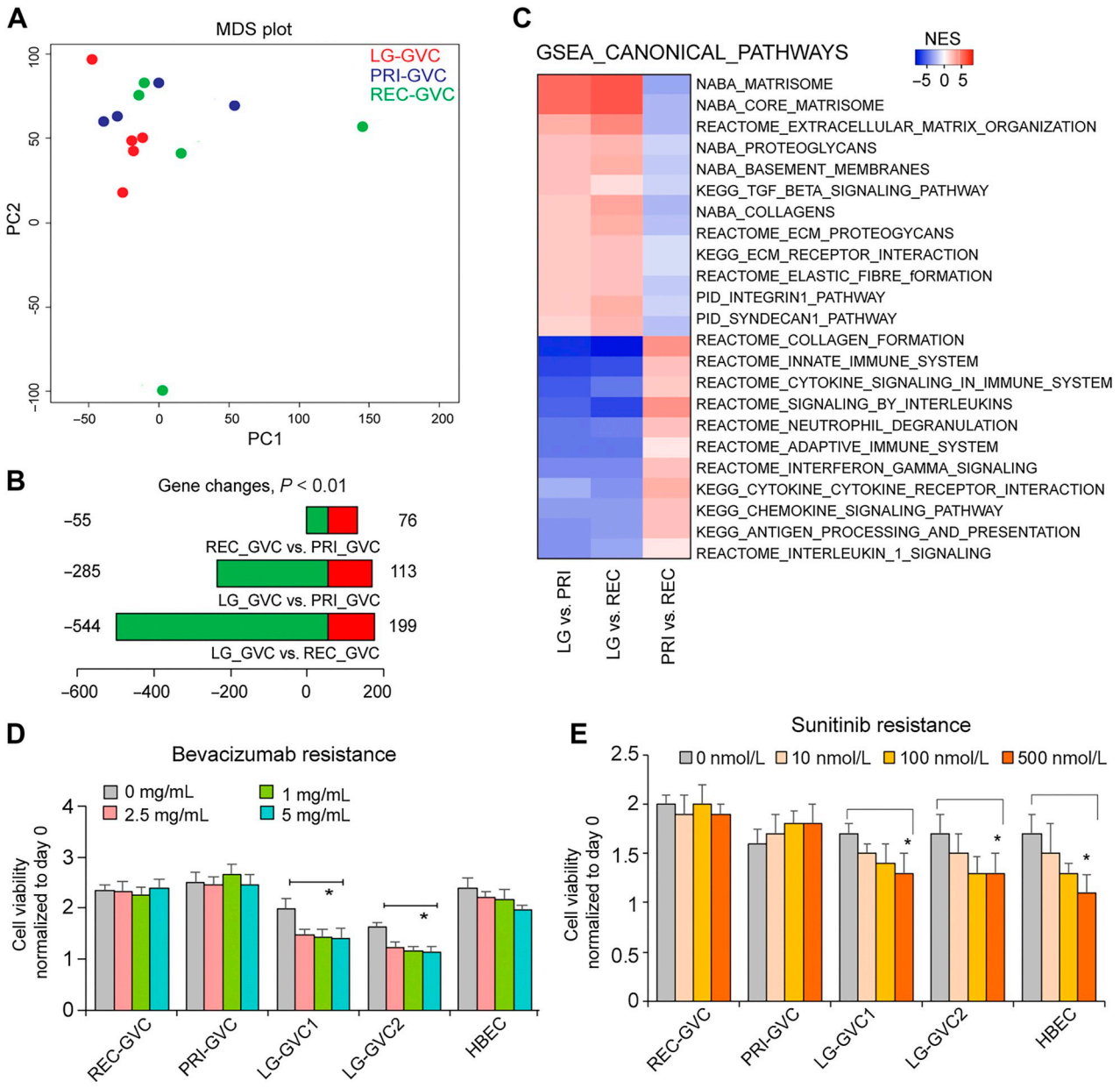

Figure 2.

Molecular and functional heterogeneity of LG- GVC and HG-GVC. **A,** MDS plot of GVC from LG-, HG (primary/PRI and recurrent/REC) gliomas. Points represent individual patient samples. **B,** Genes differentially expressed between LG- and HG-GVC. **C,** Heat map of normalized enrichment scores (NES) of canonical pathway_gene sets enriched in LG, PRI-, and REC-GVC. **D** and **E,** Normalized growth of LG, PRI-, and REC-GVC and HBEC cultured with antiangiogenic drugs bevacizumab and sunitinib. $N = 3$, *, $P < 0.05$, one-way ANOVA, post hoc t test.

found that genes enriched in LG-GVC were expressed at significantly low- or negligible levels in PRI-GVC compared with normal brain vascular cells, and genes enriched in HG-GVC were significantly upregulated in PRI-GVC corroborating the findings from cultured cells (Supplementary Fig. S4A; ref. 8). We also analyzed the expression of these genes in scRNA-seq data of $CD31^+$ endothelial cells (EC) isolated from core and edge of primary GBM tumors. LG-GVC–enriched genes (*ITIH2, WNT4, FMOD, OGN, ASPN*) showed very minimal expression in $CD31^+$ EC, whereas HG-GVC–enriched genes especially *IL1B* and *SPP1* were highly enriched in EC from both core and edge of these primary GBM tumors (Supplementary Fig. S4B and S4C; ref.13).

Next, we examined the expression of select candidates with high FPKM values in the IVY_GAP database, which primarily has expression data from HG to determine the specific histologic regions they were enriched in the tumors. *ASPN* and *NID1* were significantly higher in the microvascular proliferation regions compared with others, whereas HG-GVC–enriched chemokines *CCL18* and CXCL10 did not exhibit significant enrichment in any specific region of the tumor (Supplementary Fig. S4D). To further validate this differential

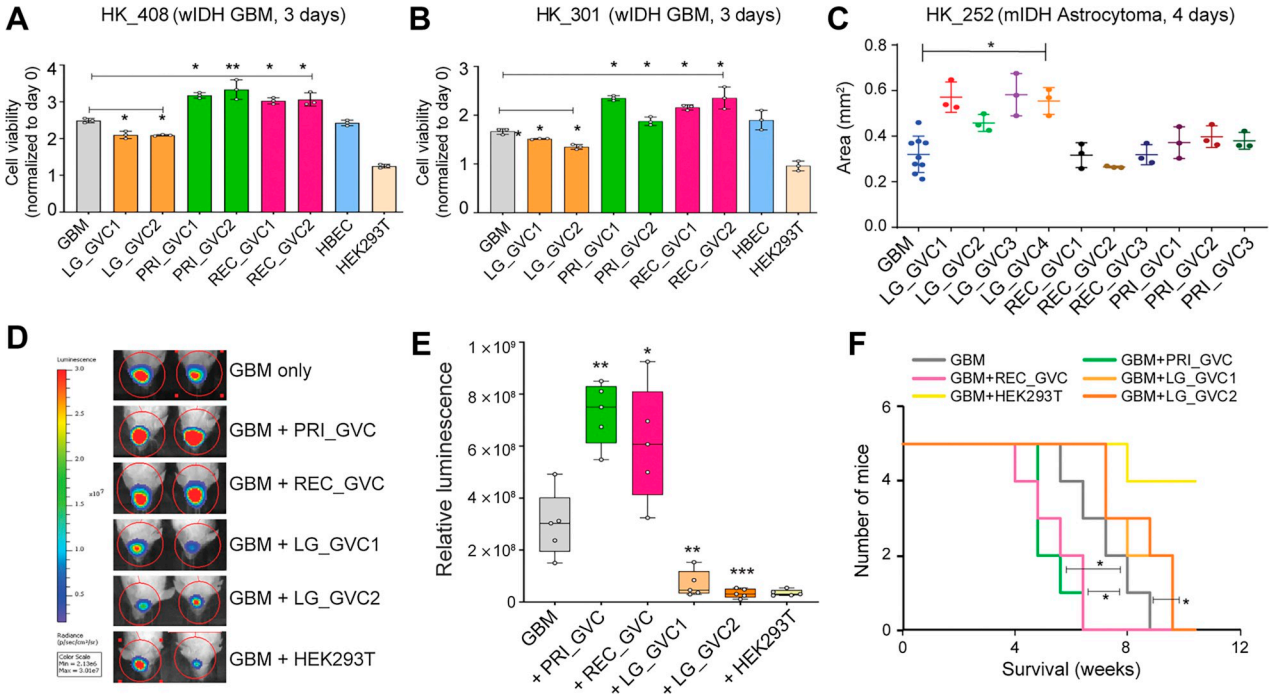

Figure 3.

LG-GVC and HG-GVC differentially regulate GBM growth. **A** and **B,** Normalized growth of wIDH GBM lines cultured in CM from LG-, PRI-, and REC-GVC and HBEC. *, $P < 0.05$; **, $P < 0.005$, one-way ANOVA. **C,** Area of mIDH astrocytoma spheroids in CM from LG-, PRI-, and REC-GVC. $N = 3$ replicates per condition. *, $P < 0.05$, one-way ANOVA. **D** and **E,** Representative bioluminescent images of tumor growth of wIDH GBM cells cotransplanted with LG-, PRI-, and REC-GVC. Box plots of relative luminescence from tumors in each condition. $N = 5$ mice per group. *, $P < 0.05$; **, $P < 0.005$; ***, $P < 0.0005$, one-way ANOVA and post hoc *t* test. **F,** Kaplan–Meier survival curve of mice cotransplanted with GBM and GVC. $N = 5$ mice per group. *, $P < 0.05$, log-rank test.

expression, we performed immunostaining on GVC cultures. As expected, ASPN and NID1 were highly expressed in LG-GVC compared with HG-GVC and HBEC. On the other hand, CCL18 and CXCL10 were expressed in HG-GVC but showed very low expression in LG-GVC and HBEC, confirming the findings from RNA-seq (**Fig. 4B**). Collectively, these data support the notion that LG- and HG-GVC are heterogeneous and show differential expression of genes including extracellular matrix proteins and cytokines.

We next tested whether these LG- and HG-GVC enriched genes differentially regulated the growth of GBM cells. Of the four candidates tested, ASPN enriched in LG-GVC significantly inhibited the growth of tumor cells ($N = 6$ wIDH GBM lines), whereas NID1 did not alter the growth of any of the tumor lines (**Fig. 4C**). CCL18 enriched in HG-GVC showed growth-enhancing effect on two GBM lines but did not alter the growth of others, and CXCL10 did not affect the growth of tumor cells (**Fig. 4D**). Based on these results, we hypothesized that the growth-inhibitory effect of LG-GVC on wIDH GBM cells is potentially mediated by ASPN.

GVC express SLC1A1 transporter and uptake D-2HG

ASPN is an extracellular matrix protein that belongs to the small-leucine-rich proteoglycan family and is reported to play both tumor-suppressive and oncogenic roles in different types of cancer (14, 15). We first confirmed that ASPN is expressed in the vessels by IHC on tumor sections obtained from grades 2/3 mIDH LG, grade 4 wIDH primary and recurrent GBM ($N = 3$ each). We also included tumor sections from grade 4 mIDH astrocytomas ($N = 3$) to assess whether ASPN expression is regulated by the IDH-mutant phenotype. We found ASPN staining in EC lining the vessels as well as in pericytes (**Fig. 5A**). Interestingly, we noted ASPN expression outside the vessels in some cells that appear like microglia (Supplementary Fig. S5A). Quantification of ASPN staining showed a significant increase in $ASPN^+$ vessels in grade 2/3 mIDH LG compared with grade 4 GBM tumors and a small yet significant increase relative to grade 4 mIDH astrocytomas (**Fig. 5B**). These results indicate that ASPN expression is enriched in LG vessels and can potentially be modulated by mIDH phenotype.

As our LG-GVC cultures were all derived from mIDH tumors, we asked if ASPN expression is regulated by d-2-hydroxyglutarate (2-HG), an oncometabolite secreted by mIDH tumor cells. A recent study reported that *SLC1A1* is expressed by human umbilical vein EC (HUVEC) and facilitates the intracellular transport of 2-HG, which promotes endothelial migration and tumor angiogenesis (16). We therefore examined our transcriptomic data to examine whether *SLC1A1* is expressed by GVC. *SLC1A1* was expressed by all GVC, whether freshly isolated from primary GBM tumors or cultured from LG- and HG tumors, as well as by normal brain EC, albeit at varying levels (**Fig. 5C**; Supplementary Fig. S5B). This suggested that GVC can uptake 2-HG from the tumor microenvironment via *SLC1A1*. We therefore treated our LG- and HG-GVC cultures with D-2HG that influxes into cells only in the presence of a transporter like *SLC1A1*. Strikingly, we observed high levels of intracellular D-2-HG in cell lysates from both LG- and HG-GVC, indicating that GVC can indeed transport D-2-HG (**Fig. 5D**).

D-2HG promotes ASPN expression in GVC

Next, we tested whether treatment of GVC with D-2HG promoted ASPN expression. qRT-PCR analysis showed that D-2HG (10 mmol/L)

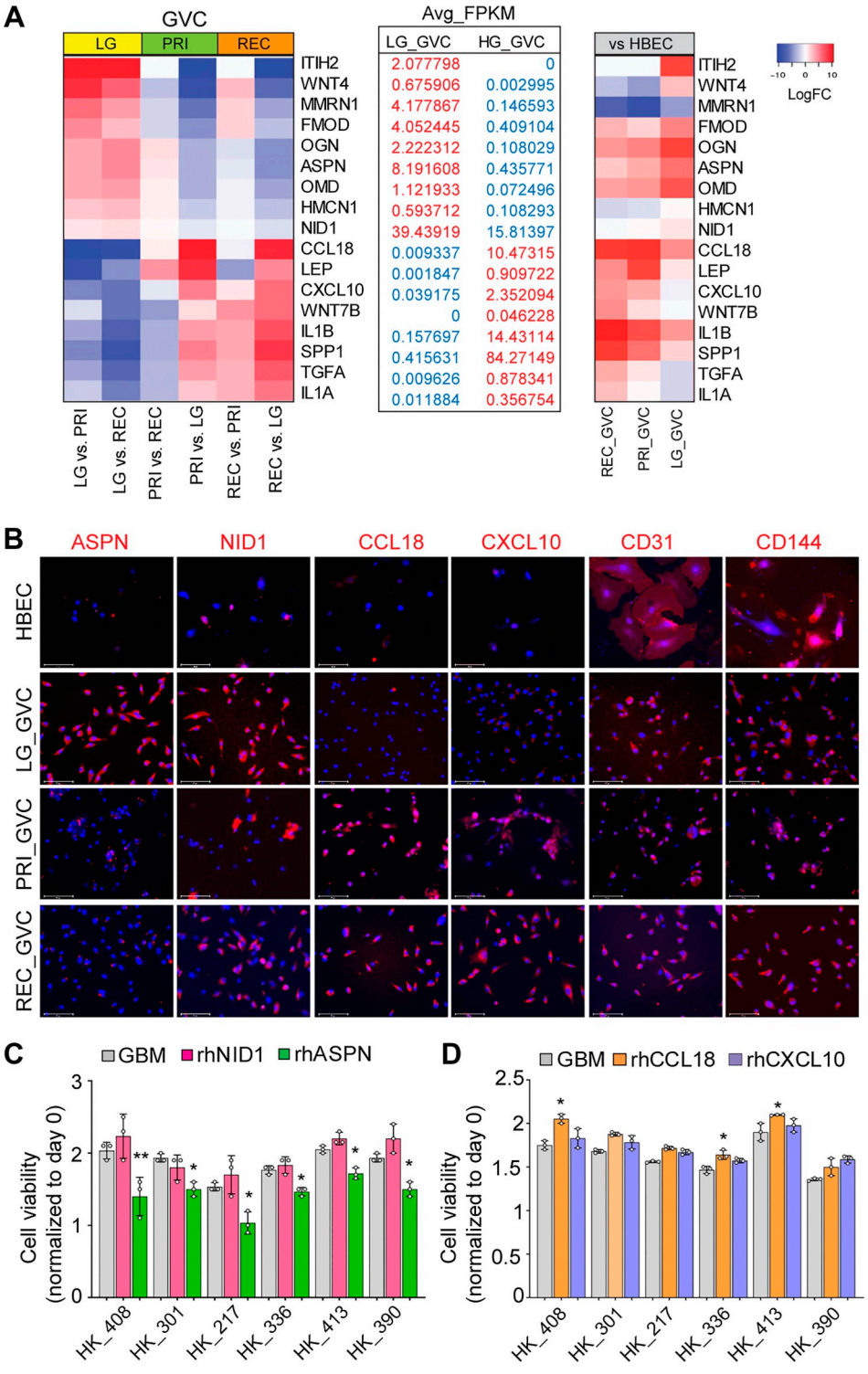

Figure 4.

LG-GVC and HG-GVC show differential expression of cytokines, chemokines, and extracellular matrix proteoglycans. **A,** Heat map of LogFC expression of significantly differentially expressed genes in LG- and HG-GVC. Average FPKM values of each gene, and LogFC expression compared with HBEC. **B,** Immunostaining of LG-GVC (ASPN, NID1) and HG-GVC enriched genes (CCL18, CXCL10) and endothelial markers (CD31 and CD144/VE-CADHERIN) in cultured GVC and HBEC. Scale bars, 125 μm. **C** and **D,** Normalized growth of wIDH GBM lines treated with recombinant NID1 and ASPN enriched in LG-GVC and CCL18 and CCL10 enriched in HG-GVC. *, $P < 0.05$; **, $P < 0.005$, one-way ANOVA.

increases *ASPN* expression in LG- and HG-GVC after 3 days of treatment, which was further confirmed by immunostaining (**Fig. 5E**; Supplementary Fig. S5C). We also performed immunoblotting of LG-GVC treated with D-2HG and detected a significant increase in *ASPN* expression (**Fig. 5F** and **G**). Additionally, we assessed whether D-2HG increases *ASPN* expression in a dose-dependent manner. We found a significant increase in *ASPN* expression with 10 mmol/L ($P = 0.03$) and 20 mmol/L ($P < 0.005$) concentrations of D-2HG, and only a small increase at 5 mmol/L ($P = 0.05$) indicating that there may be a dose-dependent effect of D-2HG on *ASPN* expression (Supplementary Fig. S5D). Furthermore, we also observed a significant increase in ASPN expression when

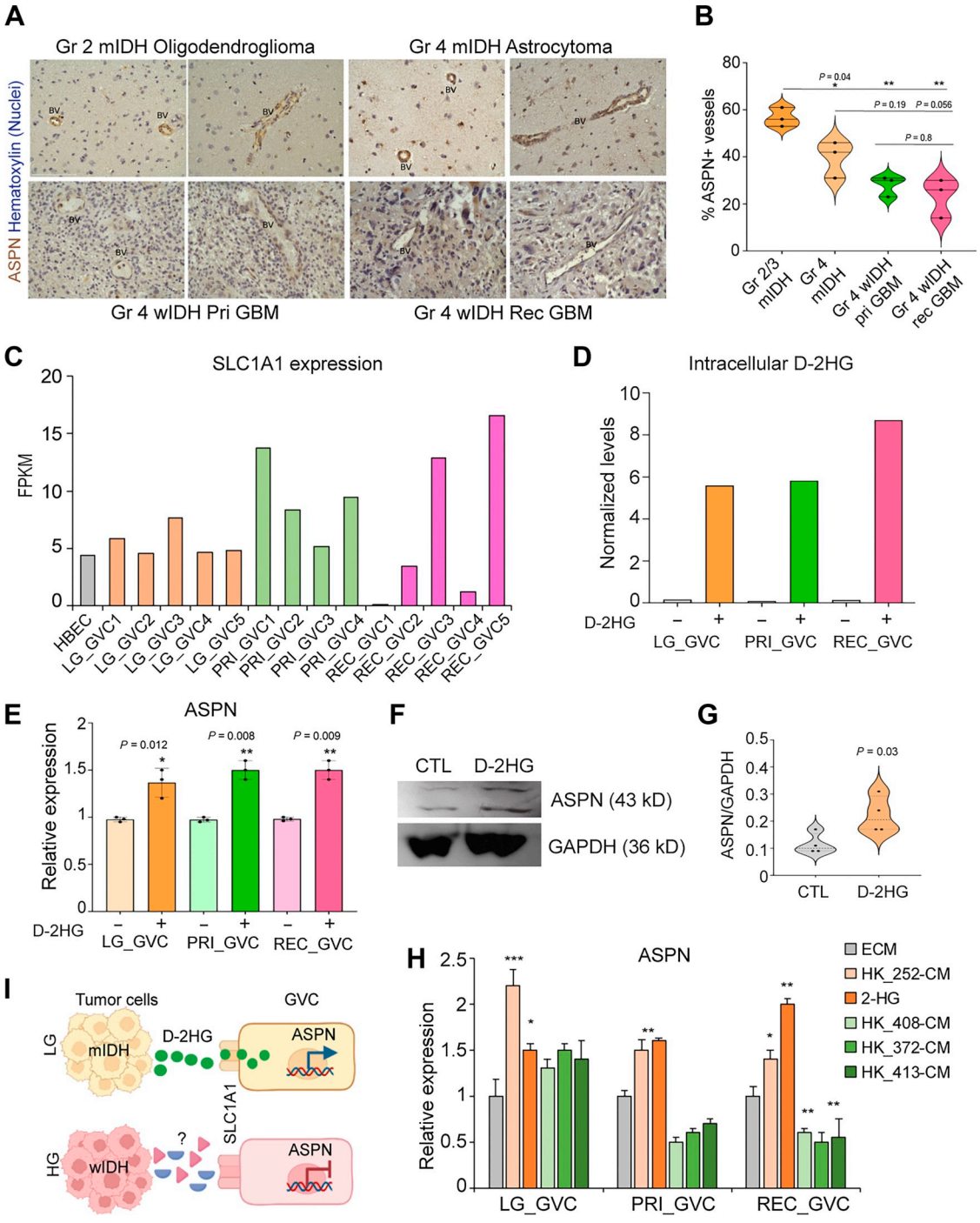

Figure 5.

ASPN is enriched in vessels from mIDH LG tumors. **A** and **B,** IHC of ASPN (brown) and hematoxylin (nuclei, blue) in tumor tissues. Scale bars, 50 μm. Quantitation of ASPN+ vessels in the tumor sections. *, $P < 0.05$ and **, $P < 0.005$, one-way ANOVA. **C,** FPKM expression of SLC1A1 in cultured HBEC and GVC. **D,** Normalized intracellular levels of D-2HG in GVC cultured for 72 hours. **E,** Relative expression of ASPN in control and D-2HG (10 mmol/L)-treated GVC. $N = 3$ independent experiments, *, $P < 0.05$ and **, $P < 0.005$, one-way ANOVA. **F** and **G,** Immunoblot of ASPN and GAPDH in control and D-2HG (10 mmol/L)-treated GVC. Quantitation of ASPN protein normalized to GAPDH. *, $P = 0.03$, unpaired t test. **H,** Relative expression of ASPN in GVC treated with 10 mmol/L 2-HG, and conditioned media (CM) from mIDH astrocytoma (252) and wIDH (408, 372, and 413) GBM cells. **I,** Schematic illustrates the putative model for differential expression of ASPN between LG- and HG-GVC.

LG- and HG-GVC were treated with CM from a mIDH grade 4 astrocytoma (HK252) line supporting the notion that 2-HG secreted by mIDH tumors promotes *ASPN* expression (**Fig. 5H**). As ASPN is expressed at relatively lower levels in HG-GVC from wIDH tumors, we wondered if GBM-secreted factors suppressed ASPN expression. HG-GVC cultured in CM from wIDH GBM ($n = 3$) lines showed a significant reduction in *ASPN* expression, whereas LG-GVC were unaffected indicating that *ASPN* expression in HG-GVC is regulated by GBM cells (**Fig. 5H**). Together, these results indicate that *ASPN* expression in GVC is differentially regulated between mIDH and wIDH tumors (**Fig. 5I**).

ASPN differentially inhibits the growth of wIDH GBM and mIDH astrocytoma

Because ASPN is differentially regulated in wIDH and mIDH tumors, and the exogenous addition of recombinant ASPN inhibited the growth of wIDH GBM lines, we asked whether it had opposing effects on the growth of wIDH and mIDH tumors. Indeed, ASPN expression significantly inhibited the growth of wIDH GBM tumor cells but had a small but significant growth-promoting effect on mIDH astrocytoma cells (**Fig. 6A**). To further confirm this, we measured EdU incorporation and found that wIDH GBM cells exposed to ASPN showed reduced proliferation whereas mIDH astrocytoma cells showed increased proliferation (**Fig. 6B** and **C**).

To functionally test if endogenous ASPN expressed by LG-GVC is required for the growth-inhibitory effects on wIDH GBM cells, we used lentiviral shRNAs to knock down ASPN. Knockdown (KD) efficiency was assessed by quantitative RT-PCR for ASPN mRNA and immunoblotting for ASPN protein (Supplementary Fig. S6A–S6C). We generated ASPN-KD and control (CTL) lines of both LG- and HG-GVC and verified by qRT-PCR (Supplementary Fig. S6D). CM from ASPN-KD cells partially rescued the growth-inhibitory effect of LG-GVC on wIDH GBM tumor cells (**Fig. 6D**). However, ASPN-KD in HG-GVC did not alter the growth of GBM cells. In addition, ASPN-KD in both LG- and HG-GVC did not significantly reduce the growth of mIDH astrocytoma cells (**Fig. 6E**). These results suggested that LG-GVC–derived ASPN elicits a growth-inhibitory effect specifically on wIDH GBM.

We next wanted to examine if ASPN inhibited the growth of wIDH GBM tumors *in vivo*. As expected, cotransplantation of LG-GVC with GBM cells significantly inhibited their growth, whereas coinjection of LG-GVC lacking ASPN with GBM cells partially rescued the growth-inhibitory effect corroborating the *in vitro* findings (**Fig. 6F**). Survival analysis also showed that mice bearing tumors with LG-GVC survived longer compared with GBM tumors only. However, mice bearing tumors with LG-GVC lacking ASPN showed reduced survival indicating that ASPN in LG-GVC is essential for the growth-inhibitory effect on GBM tumors (**Fig. 6G**). Collectively, these *in vitro* and *in vivo* findings strongly indicate that LG-GVC–derived ASPN inhibits the growth of wIDH GBM tumors.

ASPN inhibits wIDH GBM growth by modulating TGFβ1 signaling

To determine the potential mechanism by which ASPN regulates wIDH GBM growth, we performed RNA-seq on 72 hours of ASPN-treated wIDH GBM (HK408) and mIDH astrocytoma (HK252) cells. Differential expression analysis revealed a small number of genes regulated by ASPN in wIDH GBM, but a significantly greater number of genes in mIDH astrocytoma cells (**Fig. 7A**). Of the top differentially expressed genes, most transcripts upregulated by ASPN in wIDH GBM were diminished in the mIDH tumor cells. Similarly, several transcripts downregulated by ASPN in wIDH GBM were either upregulated or showed no significant change in the mIDH tumor cells (**Fig. 7B**). Gene Ontology analysis showed that ASPN enriched for GPCR signaling and downregulated TGFβ1 and ALK signaling in wIDH GBM cells, and conversely, upregulated these pathways in mIDH tumor cells (**Fig. 7C**).

ASPN has been previously reported to regulate TGFβ1 signaling (14, 15). Consistent with this notion, we found that SMAD6, a TGFβ1 target gene, was downregulated in wIDH GBM and upregulated in mIDH tumor cells (**Fig. 7C** and **D**). *GPM6A*, a highly enriched transcript in wIDH GBM upon ASPN treatment, was previously reported to be suppressed by TGFβ1 signaling in mesothelial cells (17). In addition, GPM6A is known to regulate MAPK signal transduction and recycling of GPCRs, and these pathways were increased with ASPN treatment in wIDH GBM (**Fig. 7C**; Supplementary Fig. S7A; ref. 18). Based on these data, we hypothesized that ASPN inhibits the growth of wIDH GBM by modulating the TGFβ1-GPM6A axis.

To determine if TGFβ1 signaling regulates GBM growth, we treated wIDH GBM and mIDH astrocytoma cells with recombinant TGFβ1 either alone or in combination with recombinant ASPN. As expected, TGFβ1 treatment promoted growth, and the addition of ASPN reversed this effect in wIDH GBM (**Fig. 7E**). On the contrary, TGFβ1 did not have a significant effect on the growth of mIDH astrocytoma cells (**Fig. 7F**). We further confirmed this effect by measuring proliferation using EdU incorporation assay (**Fig. 7G** and **H**). We also verified that TGFβ1 signaling was activated by immunostaining for pSMAD2/3 in wIDH and mIDH cells (Supplementary Fig. S7B). Moreover, we found that ASPN inhibited the expression of SMAD2/3 target genes including *SMAD6, SMAD7*, and *ID1* downstream of TGFβ1 in wIDH GBM cells (Supplementary Fig. S7C). Together, these results indicated that ASPN antagonizes TGFβ1 signaling and its growth-promoting effect on wIDH GBM.

Knockdown of GPM6A rescues the growth-inhibitory effect of ASPN in wIDH GBM

To determine whether there is an inverse relationship between TGFβ1 and *GPM6A* downstream of ASPN, we measured the expression of *GPM6A* in TGFβ1- and ASPN-treated wIDH GBM cells. As expected, ASPN increased and TGFβ1 strongly inhibited the expression of *GPM6A*. The inhibitory effect of TGFβ1 on GPM6A expression was reversed by cotreatment with ASPN (**Fig. 7I**). This supported our hypothesis that ASPN antagonizes TGFβ1 signaling to promote *GPM6A* expression and inhibits wIDH GBM growth.

Next, we asked whether we could rescue the growth-inhibitory effect of ASPN by blocking *GPM6A* expression. *GPM6A* knockdown in wIDH GBM and mIDH tumor cells was performed using shRNA constructs. Knockdown efficiency was validated by qRT-PCR and immunostaining (Supplementary Fig. S7D and S7E). Interestingly, *GPM6A*-KD alone did not have significant effects on the growth of either wIDH or mIDH tumor cells. However, GPM6A-KD rescued the growth inhibition of ASPN in wIDH GBM but had no effect in mIDH tumor cells (**Fig. 7J**; Supplementary Fig. S7F). These results indicate that GPM6A is essential for ASPN-mediated suppression of wIDH GBM growth. Collectively, our findings indicate that low-grade TEC-derived ASPN inhibits the growth and proliferation of wIDH GBM cells by regulating the TGFβ1-GPM6A axis (**Fig. 7K**).

Discussion

Early transcriptomic profiling studies reported that vascular cells from LG and HG exhibit significant phenotypic and molecular differences from normal brain EC (5, 6, 11). More recent scRNA-seq studies

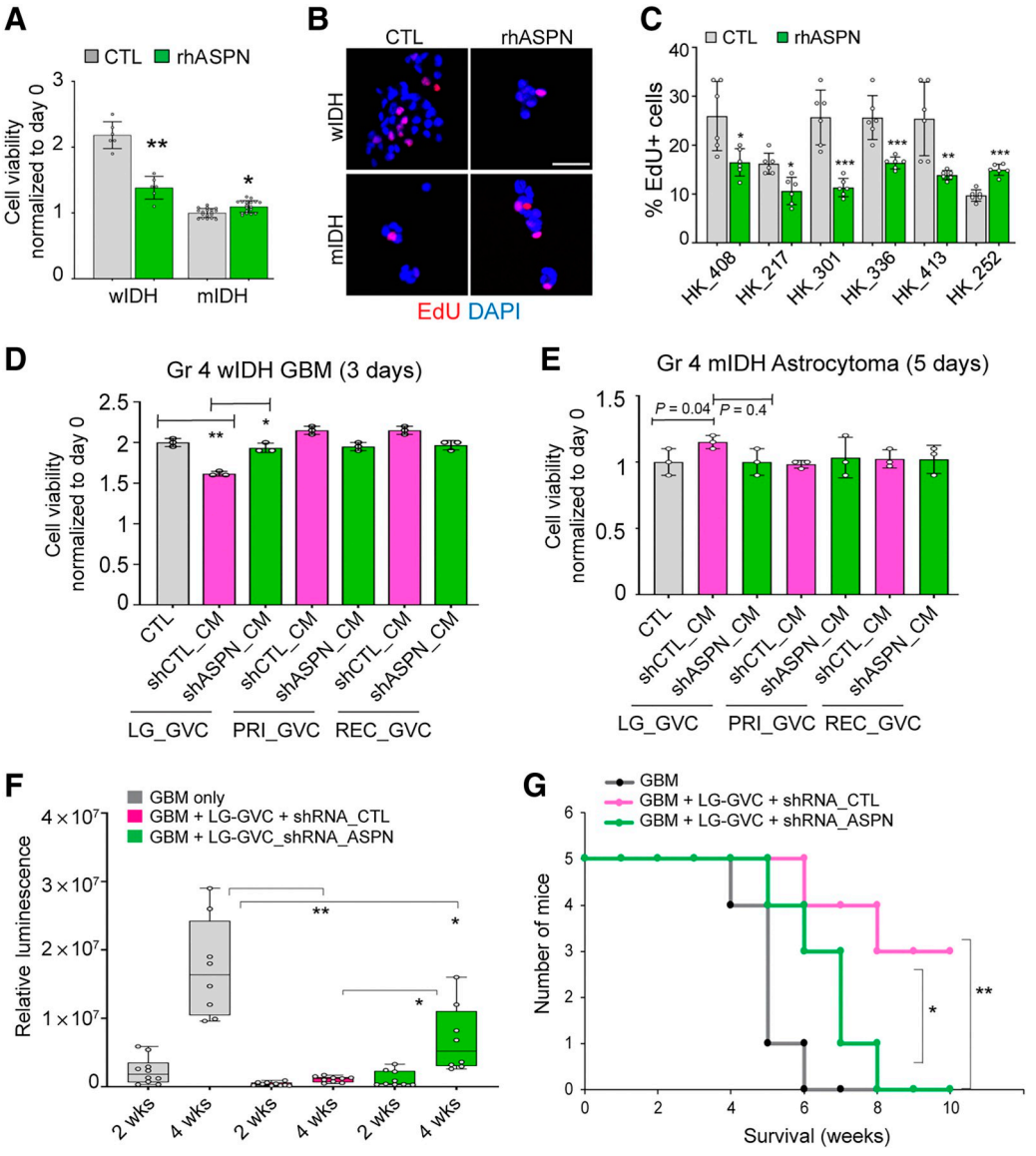

Figure 6.

ASPN differentially controls the growth of mIDH astrocytoma and wIDH GBM. **A,** Normalized growth of wIDH GBM and mIDH astrocytoma cells treated with recombinant ASPN (100 ng/mL). *, $P < 0.05$; **, $P < 0.005$, unpaired *t* test. **B,** Representative images of EdU (red) incorporation in wIDH GBM and mIDH astrocytoma cells treated with ASPN. Scale bars, 50 μm. **C,** Quantitation of the percentage of EdU^+ cells in wIDH GBM (408, 217, 301, 336, 413) and mIDH (252) tumor cells. *, $P < 0.05$; **, $P < 0.005$; ***, $P < 0.0005$, unpaired *t* test. **D,** Normalized growth of wIDH GBM cells treated with CM from shRNA-CTL or shRNA-ASPN infected GVC. *, $P < 0.05$; **, $P < 0.005$, one-way ANOVA. **E,** Normalized growth of mIDH tumor cells treated with conditioned media from shRNA-CTL or shRNA-ASPN infected GVC. $P = 0.04$, one-way ANOVA. **F,** Box plots show relative luminescence from tumors in each condition at 2 and 4 weeks posttransplantation. $N = 5$ mice per group. *, $P < 0.05$; **, $P < 0.005$, one-way ANOVA and post hoc *t* test. **G,** Kaplan–Meier survival curve of mice co–transplanted with wIDH GBM and LG-GVC infected with shRNA-CTL or shRNA-ASPN. $N = 5$ mice per group, *, $P < 0.05$, log-rank test.

demonstrated that $CD31^+$ EC derived from the core and edge of primary GBM tumors exhibit intratumoral heterogeneity, as well as from transdifferentiated ECs (7, 13). These studies, while being a valuable resource, have not yielded insights into specific mechanisms by which vascular cell heterogeneity contributes to tumor growth and resistance.

In this study, we established $CD31^+$ vascular cell cultures from grade 2/3 mIDH LG and grade 4 wIDH HG (GBM) tumors to not only elucidate their molecular heterogeneity but also understand how this heterogeneity influences tumor growth and progression. By performing extensive transcriptomic sequencing of these cultured LG- and HG-GVC and HBECs, we identified key molecular differences in their expression of extracellular matrix proteins, growth factors, and cytokines. We also demonstrated that a few of these differentially expressed factors have distinct effects on the growth and proliferation of GBM cells derived from wIDH and mIDH tumors. This indicated that the mechanisms by which GVC control tumor growth may be different in LG versus HG and also dependent on the mutational status of the tumors as previously indicated (11).

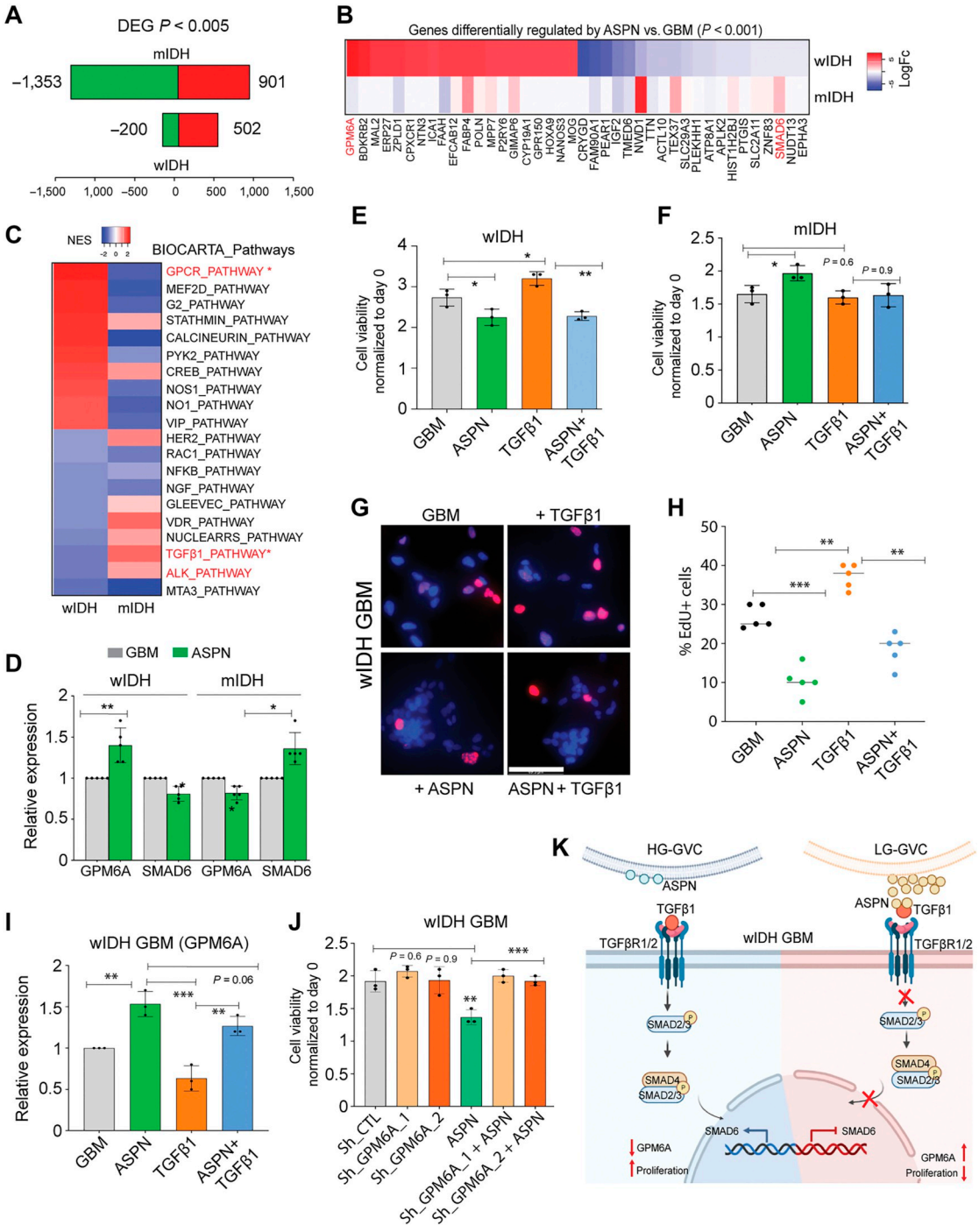

Figure 7.

ASPN inhibits the growth of wIDH GBM via TGFβ1-GPM6A signaling. **A,** Differentially expressed genes in wIDH GBM and mIDH astrocytoma-treated with ASPN (100 ng/mL) for 72 hours. **B,** Heat map of ASPN-regulated genes between mIDH astrocytoma and wIDH GBM cells. **C,** Heat map shows differentially regulated pathways between mIDH and wIDH tumor cells. **D,** Relative expression of GPM6A and SMAD6 in mIDH and wIDH tumor cells treated with ASPN. *, $P < 0.05$; **, $P < 0.005$, unpaired *t* test. **E,** Normalized growth of wIDH cells treated with ASPN, TGFβ1 (10 ng/mL) alone or in combination for 3 days. *, $P < 0.05$; **, $P < 0.005$, one-way ANOVA. **F,** Normalized growth of mIDH tumor cells treated with ASPN, TGFβ1 alone or in combination for 5 days. *, $P < 0.05$, derived from one-way ANOVA. **G,** Representative images of EdU (red) incorporation in wIDH GBM cells treated with ASPN, TGFβ1 alone or in combination for 3 days. Scale bars, 69.3 μm. **H,** Quantitation of the percentage of EdU+ cells in wIDH (408, 217, 301, 336, and 413) and mIDH (252) tumor cells. **, $P < 0.005$; ***, $P < 0.0005$, one-way ANOVA. **I,** Relative expression of GPM6A in wIDH GBM cells treated with ASPN and TGFβ1 alone or in combination. **, $P < 0.005$; ***, $P < 0.0005$, one-way ANOVA. **J,** Normalized growth of shRNA-CTL and shRNA-ASPN infected wIDH GBM cells treated with ASPN for 3 days. **, $P < 0.005$; ***, $P < 0.0005$, one-way ANOVA. **K,** Schematic of the model of differential regulation of TGFβ1 signaling and growth of wIDH GBM by LG- and HG-GVC.

LG- and HG-GVC exhibit significant functional differences in their response to antiangiogenic drugs, bevacizumab (BVZ) and sunitinib. In line with prior findings, HG-GVC are resistant to both antiangiogenic treatments, whereas LG-GVC are sensitive to these drugs (19). Although these therapies have failed in improving overall patient survival outcomes for GBM tumors, they may still hold some promise for mIDH LG gliomas and warrant further investigation.

Prior research indicated that radiotherapy disrupts the vasculature and exerts a broad range of effects including endothelial senescence, increased inflammation, immune cell recruitment and revascularization of the tumor (20, 21). Here, we found that both LG- and HG-GVC are resistant to high doses of radiation and proliferate like nonradiated cells. However, our analysis was limited to assessing proliferation for only a short duration of 3 days, and we did not assess the extent of DNA damage in GVC. Further experiments are needed to elucidate whether GVC are refractory to radiation in long-term culture or undergo senescence and display adaptive resistance. In addition, it remains undetermined how antiangiogenic, radiation, or chemotherapy alters the molecular landscape of GVC and in turn influences tumor growth.

A major and unexpected finding of this study is that LG-GVC–derived factors have differential effects on the growth of wIDH and mIDH tumors. Although we validated the growth-inhibitory effect of LG-GVC on wIDH tumors *in vivo* in cotransplantation studies, we were not successful in growing mIDH tumors in orthotopic xenograft models. There is an unmet need in GBM research to develop methods to effectively transplant and grow LG and HG mIDH tumors *in vivo*.

Our DEA revealed ASPN as highly enriched in the mIDH LG-GVC relative to wIDH HG-GVC. ASPN expression is dysregulated in several cancers and has been reported to act as an oncogene in pancreatic, colorectal, gastric, and prostate cancer, and as a tumor suppressor in triple-negative breast cancer (22). Moreover, it regulates several signaling pathways including TGFβ, EGFR, and CD44 pathways to control tumor proliferation, migration, and invasion (22). The functional role of ASPN has not been previously described in GBM or its expression in glioma vasculature. However, prior studies have indicated that *ASPN* transcript is enriched in normal brain mural cells or pericytes (23, 24). Our immunostaining experiments indicate that ASPN is strongly expressed by both endothelial cells and pericytes in the tumor vessels, predominantly in mIDH tumors. In addition, we also found ASPN expression in cells with extensive processes suggestive of microglia indicating that its expression may not be restricted to the vasculature. Our data also suggested that ASPN expression is regulated by 2-hydroxyglutarate (2-HG), an oncometabolite secreted by mIDH tumors. *ASPN* expression in HG-GVC was suppressed by treatment with CM of wIDH tumor cells, but expression in LG-GVC was not affected. Our findings indicate that ASPN acts as a tumor suppressor for mIDH tumors, and that its expression is differentially regulated in GVC from mIDH LG and wIDH HG tumors. The specific mechanism by which *ASPN* expression is suppressed in HG-GVC, and what other functions it may serve in GBM biology remains to be determined. Moreover, knockdown of ASPN in LG-GVC only partially rescued the growth-inhibitory effect of LG-GVC on wIDH tumor cells indicating that LG-GVC may influence the growth and proliferation of tumor cells via multiple mechanisms. However, we speculate that inhibition of ASPN expression is a prerequisite to the establishment or progression of GBM.

ASPN treatment differentially altered the transcriptional landscape of wIDH and mIDH tumors. Several genes upregulated by ASPN in wIDH GBM cells are diminished in expression in mIDH tumor cells including TGFβ1 and GPCR pathway-associated genes. Glycoprotein M6A (*GPM6A*), the most significantly upregulated gene in wIDH GBM cells, is markedly downregulated in mIDH tumor cells upon ASPN treatment. On the other hand, *SMAD6*, a downstream target of TGFβ1 signaling, is downregulated by ASPN in wIDH GBM but enhanced in mIDH tumor cells indicating that ASPN differentially influences these signaling pathways in IDH-wild-type and mutant glioma cells. TGFβ1 was previously reported to modulate the expression of *GPM6A* in mesothelial cells of the liver (25). In line with this, our findings also show that TGFβ1 treatment reduces GPM6A expression, whereas ASPN increases *GPM6A* by blocking TGFβ1 signaling in wIDH GBM cells. Furthermore, GPM6A knockdown rescues the growth-inhibitory effect of ASPN in wIDH GBM cells but has no effect on mIDH tumor cells suggesting that they all function in a single axis to control growth of wIDH GBM cells. One potential advantage of suppressing ASPN expression in HG-GVC by wIDH GBM cells could be that it regulates TGFβ1 signaling, a known effector signaling molecule of immunosuppression that aids in tumor cell escape from immune surveillance and promotes tumor growth and progression (26). Future studies will be needed to investigate whether ASPN overexpression blocks TGFβ1 signaling in GBM tumors.

In conclusion, our study revealed the molecular and functional heterogeneity between LG- and HG-GVC and identified ASPN expressed by mIDH LG-GVC as a potential regulator of TGFβ1 signaling–mediated GBM tumor growth.

Authors' Disclosures

No disclosures were reported.

Authors' Contributions

S.D. Muthukrishnan: Conceptualization, formal analysis, validation, investigation, visualization, methodology, writing–original draft, writing–review and editing. **H. Qi:** Formal analysis, investigation, visualization. **D. Wang:** Investigation. **L. Elahi:** Formal analysis, investigation, visualization, methodology. **A. Pham:** Formal analysis, investigation, visualization. **A.G. Alvarado:** Investigation. **T. Li:** Investigation, methodology. **F. Gao:** Data curation, formal analysis. **R. Kawaguchi:** Data curation, software, formal analysis, methodology. **A. Lai:** Resources. **H.I. Kornblum:** Conceptualization, resources, supervision, funding acquisition, project administration, writing–review and editing.

Acknowledgments

This work was supported by grants from the Dr. Miriam and Sheldon G. Adelson Medical Research Foundation (H.I. Kornblum), UCLA SPORE in Brain Cancer P50 CA211015 (H.I. Kornblum), The NIH grant RO1 NS121617 (H.I. Kornblum). The authors thank the UCLA BTTR, JCCC Flow Cytometry Core, UNGC, and the TCGB core for technical contributions.

Note

Supplementary data for this article are available at Molecular Cancer Research Online (http://mcr.aacrjournals.org/).

Received December 22, 2023; revised February 13, 2024; accepted March 1, 2024; published first March 5, 2024.

References

1. Zhang AB, Mozaffari K, Aguirre B, Li V, Kubba R, Desai NC, et al. Exploring the past, present, and future of anti-angiogenic therapy in glioblastoma. Cancers 2023;15:830.
2. Hardee ME, Zagzag D. Mechanisms of glioma-associated neovascularization. Am J Pathol 2012;181:1126–41.
3. Peleli M, Moustakas A, Papapetropoulos A. Endothelial-tumor cell interaction in brain and CNS malignancies. Int J Mol Sci 2020;21:7371.
4. Charalambous C, Chen TC, Hofman FM. Characteristics of tumor-associated endothelial cells derived from glioblastoma multiforme. FOC 2006;20:E22.
5. Dieterich LC, Mellberg S, Langenkamp E, Zhang L, Zieba A, Salomäki H, et al. Transcriptional profiling of human glioblastoma vessels indicates a key role of VEGF-A and TGFβ2 in vascular abnormalization. J Pathol 2012;228:378–90.
6. Dusart P, Hallström BM, Renné T, Odeberg J, Uhlén M, Butler LM. A systems-based map of human brain cell-type enriched genes and malignancy-associated endothelial changes. Cell Rep 2019;29:1690–706.
7. Carlson JC, Cantu Gutierrez M, Lozzi B, Huang-Hobbs E, Turner WD, Tepe B, et al. Identification of diverse tumor endothelial cell populations in malignant glioma. Neuro-oncol 2021;23:932–44.
8. Ghochani Y, Muthukrishnan SD, Sohrabi A, Kawaguchi R, Condro MC, Bastola S, et al. A molecular interactome of the glioblastoma perivascular niche reveals integrin binding sialoprotein as a mediator of tumor cell migration. Cell Rep 2022;41:111511.
9. Wojtukiewicz MZ, Mysliwiec M, Matuszewska E, Sulkowski S, Zimnoch L, Politynska B, et al. Heterogeneous expression of proangiogenic and coagulation proteins in gliomas of different histopathological grade. Pathol Oncol Res 2021;27:605017.
10. Mellinghoff IK, Chang SM, Jaeckle KA, van den Bent M. Isocitrate dehydrogenase mutant grade II and III glial neoplasms. Hematol Oncol Clin North Am 2022;36:95–111.
11. Zhang L, He L, Lugano R, Roodakker K, Bergqvist M, Smits A, et al. IDH mutation status is associated with distinct vascular gene expression signatures in lower-grade gliomas. Neuro-oncol 2018;20:1505–16.
12. Muthukrishnan SD, Kawaguchi R, Nair P, Prasad R, Qin Y, Johnson M, et al. P300 promotes tumor recurrence by regulating radiation-induced conversion of glioma stem cells to vascular-like cells. Nat Commun 2022;13:6202.
13. Xie Y, He L, Lugano R, Zhang Y, Cao H, He Q, et al. Key molecular alterations in endothelial cells in human glioblastoma uncovered through single-cell RNA sequencing. JCI Insight 2021;6:e150861.
14. Maris P, Blomme A, Palacios AP, Costanza B, Bellahcène A, Bianchi E, et al. Asporin is a fibroblast-derived TGF-β1 inhibitor and a tumor suppressor associated with good prognosis in breast cancer. PLoS Med 2015;12:e1001871.
15. Li H, Zhang Z, Chen L, Sun X, Zhao Y, Guo Q, et al. Cytoplasmic asporin promotes cell migration by regulating TGF-β/Smad2/3 pathway and indicates a poor prognosis in colorectal cancer. Cell Death Dis 2019;10:109.
16. Wang X, Chen Z, Xu J, Tang S, An N, Jiang L, et al. SLC1A1-mediated cellular and mitochondrial influx of R-2-hydroxyglutarate in vascular endothelial cells promotes tumor angiogenesis in IDH1-mutant solid tumors. Cell Res 2022;32:638–58.
17. Li Y, Lua I, French SW, Asahina K. Role of TGF-β signaling in differentiation of mesothelial cells to vitamin A-poor hepatic stellate cells in liver fibrosis. Am J Physiol Gastrointest Liver Physiol 2016;310:G262–72.
18. León A, Aparicio GI, Scorticati C. Neuronal glycoprotein M6a: an emerging molecule in chemical synapse formation and dysfunction. Front. Synaptic Neurosci. 2021;13:661681.
19. Borovski T, Beke P, van Tellingen O, Rodermond HM, Verhoeff JJ, Lascano V, et al. Therapy-resistant tumor microvascular endothelial cells contribute to treatment failure in glioblastoma multiforme. Oncogene 2013;32:1539–48.
20. Berg TJ, Pietras A. Radiotherapy-induced remodeling of the tumor microenvironment by stromal cells. Semin Cancer Biol 2022;86:846–56.
21. Seo Y-S, Ko IO, Park H, Jeong YJ, Park J-A, Kim KS, et al. Radiation-induced changes in tumor vessels and microenvironment contribute to therapeutic resistance in glioblastoma. Front Oncol 2019;9:1259.
22. Zhan S, Li J, Ge W. Multifaceted roles of asporin in cancer: current understanding. Front Oncol 2019;9:948.
23. He L, Vanlandewijck M, Raschperger E, Andaloussi Mäe M, Jung B, Lebouvier T, et al. Analysis of the brain mural cell transcriptome. Sci Rep 2016;6:35108.
24. Oudenaarden C, Sjölund J, Pietras K. Upregulated functional gene expression programmes in tumour pericytes mark progression in patients with low-grade glioma. Molecular Oncology 2022;16:405–21.
25. Lua I, Li Y, Pappoe LS, Asahina K. Myofibroblastic conversion and regeneration of mesothelial cells in peritoneal and liver fibrosis. Am J Pathol 2015;185:3258–73.
26. Han J, Alvarez-Breckenridge CA, Wang Q-E, Yu J. TGF-β signaling and its targeting for glioma treatment. Am J Cancer Res 2015;5:945–55.